

2023

Silver Doped Nanoceria (AgCNP) Integrated Silk Scaffold For Chronic Wound Healing

Architha K. Venkatesan
University of Central Florida

 Part of the [Biology and Biomimetic Materials Commons](#)

Find similar works at: <https://stars.library.ucf.edu/honorsthesis>

University of Central Florida Libraries <http://library.ucf.edu>

This Open Access is brought to you for free and open access by the UCF Theses and Dissertations at STARS. It has been accepted for inclusion in Honors Undergraduate Theses by an authorized administrator of STARS. For more information, please contact STARS@ucf.edu.

Recommended Citation

Venkatesan, Architha K., "Silver Doped Nanoceria (AgCNP) Integrated Silk Scaffold For Chronic Wound Healing" (2023). *Honors Undergraduate Theses*. 1431.
<https://stars.library.ucf.edu/honorsthesis/1431>

SILVER DOPED NANOCERIA (AGCNP) INTEGRATED SILK SCAFFOLD
FOR CHRONIC WOUND HEALING

by

ARCHITHA KRISHNAMMAL VENKATESAN

A thesis submitted in partial fulfillment of the requirements
for the Honors Undergraduate Thesis Program in Material Sciences and Engineering
in the College of Computer Science and Engineering and in the Burnett Honors College
at the University of Central Florida Orlando, Florida

Spring Term

2023

Thesis Chair: Dr. Sudipta Seal

ABSTRACT

Chronic wound healing can be seriously impeded by the formation of biofilms, infections, peri-wound edema, hematoma, osteomyelitis, and the formation of reactive oxidative species (ROS). We hypothesize that a scaffold created from Silver-Doped Nanoceria (AgCNP) embedding silk can be beneficial to aid the wound healing process, inhibit inflammation and prevent microorganisms from forming a biofilm over the wound. Current wound healing methods such as intradermal injections are not advantageous to use since they can cause unwanted responses elsewhere in the body other than the wound site. Silk, however, has a positive impact on the wound healing effect and can be used as an alternative delivery method to deliver the drugs to the target site rather than intradermal injections since its degradability is controllable and it is bioresorbable, therefore it can get absorbed by the body and degrade safely without causing bodily harm. AgCNPs are used as they have antimicrobial/antioxidant properties to scavenge harmful ROS species at the wound site and can also modify silk for UV protection. As silk's degradability can be controlled, our experiment will involve collecting data on release studies conducted in vitro to see how long it takes for the silk patch to release the drugs. Our goal is to ensure the drug is not released immediately but rather over a longer controlled time manner to protect the wound while healing.

ACKNOWLEDGMENTS

I would first like to thank my thesis chair Dr. Sudipta Seal, and my in-lab supervisor Dr. Elayaraja Kolanthai for being my mentors during my journey through this research project. I would also like to thank my thesis committee members, Dr. Melanie Coathup and Dr. Ellen Kang, for their valuable insights to help form my thesis proposal. I also wish to thank the graduate students in lab who had helped me on top of their busy schedule with my work when I had questions or needed assistance. Without the help of everyone, this research would not be possible. Lastly, I extend my sincere thanks to my family and friends for their endless support throughout my academic journey.

TABLE OF CONTENTS

1. INTRODUCTION.....	1
1.1 Challenges in Chronic Wound Healing.....	1
1.2 The Wound Healing Mechanism	3
1.3 Silk for Wound Healing.....	4
1.4 Silver Nanoparticles for Wound Healing.....	4
1.5 Cerium Oxide for Wound Healing	5
1.6 A Potential Solution for Enhancing Chronic Wound Healing.....	6
2. EXPERIMENTAL METHODS.....	8
2.1 Silk Solution Preparation	8
2.2 Nanoparticle Synthesis	11
2.3 Silk Composite Preparation Using Electrospinning	11
2.4 Nanoparticle Characterization	11
2.5 Silk Composites Characterization	12
3. RESULTS AND DISCUSSION	13
3.1 Sample Preparation	13
3.2 Nanoparticle Characterization Results.....	14
3.3 Silk Composites Characterization Results.....	16
4. CONCLUSION	22
5. REFERENCES.....	23

TABLE OF FIGURES

Figure 1. Schematic representation of the wound healing process	4
Figure 2. Diagram for proposed silk patch embedded with silver doped nanoceria particles..	7
Figure 3. Schematic diagram for silk patch sample preparation	10
Figure 4. Control silk patch created using electrospinning.....	14
Figure 5. Results of XPS analysis for CNPs and AgCNPs.....	14
Figure 6. Results of UV/Vis analysis for CNPs and AgCNPs.....	15
Figure 7. TEM Images for CNP and AgCNP	16
Figure 8. Results of XPS analysis for Silk and Silk Composite	17
Figure 9. MTT Assay was conducted using all three silk scaffolds	18
Figure 10. Scratch Assay is conducted on all three silk composites.....	19

1. INTRODUCTION

1.1 Challenges in Chronic Wound Healing

A problem facing healthcare today is the increasing incidence of chronic wounds and a deficit of adequate wound healing methods. Chronic wounds are injuries to the skin or underlying tissue that do not progress efficiently through the wound healing phases in a timely manner. Multiple factors can affect different phases of wound healing causing the process to be seriously impeded. Factors that can negatively affect the wound healing process include formation of biofilms, infections, persistent inflammation, reduced blood flow, peri-wound edema, hematoma, osteomyelitis, and the formation of reactive oxidative species (ROS) (S. Guo & L.A. Dipietro, 2010). These factors can stem from conditions such as diabetes and obesity, usage of medications like steroids and non-steroidal anti-inflammatory drugs, oncological treatments such as radiation therapy and chemotherapy, and lifestyle habits like smoking and alcohol consumption are all examples of co-morbidities that can have a negative impact on the healing of wounds. For example, a common complication seen in diabetic patients is peripheral arterial disease which can lead to a decrease in the blood flow to the wound site impeding the healing process due to reduced levels of oxygen and nutrition available. Another example is smoking nicotine which not only reduces blood flow by inducing vasoconstriction, but also results in the production of proteases that lead to further tissue destruction and immune system suppression greatly increasing the likelihood of contracting an infection at the wound site. The impact of factors impeding wound healing may impede the proper progression of wound healing, making the wound site more susceptible to unwanted pathologies from foreign pathogens (K. Anderson & R.L. Hamm, 2014).

This thesis focuses on one significant obstacle that impedes efficient wound healing, which is formation of biofilms at the wound site. Biofilm formation is a challenge facing chronic wound healing as it impedes the wound healing process. This issue is seen in over 60% of chronic wounds and is an adverse issue. Biofilms consist of more than one species of microbe and therefore are greatly resistant to host immune responses and less susceptible to antibiotic therapy. Biofilms can cause chronic infection of the wound site which are highly dangerous (S. Darvishi et al., 2022). In bacterial biofilms, bacteria can cluster to the surface of the wound site and synthesize a film layer around themselves in a hydrated polymeric matrix. This layer allows the bacteria to easily develop resistance to antibacterial therapies and the body's immune system to multiply successfully (J.W. Costerton, P.S. Stewart, & E.P. Greenberg, 1999). The extent of microbial presence in biofilms can be highly associated with the severity of chronic wounds. Greater microbial presence in biofilms may signify more severe chronic wounds. However, diagnosing chronic wound biofilms can be challenging, and research is ongoing to determine potential treatments. Promising therapies for chronic wounds include the utilization of nanobiotechnological based therapy, ultrasonic debridement, antiseptic remedies, antibiotic remedies, antimicrobial peptide treatment, photodynamic therapy, and biodegradable bacterial by-products (F. Diban et al., 2023). To better understand the various therapies available for chronic wound healing, it is important to understand the four stages involved in the wound healing process. Understanding the four stages involved in the wound healing process is important because it can help healthcare professionals to properly manage chronic wounds and optimize the use of these therapies.

1.2 The Wound Healing Mechanism

As illustrated in Figure 1, there are four stages involved in the progression of the proper wound healing process. These stages can overlap with one another but generally occur in a successive order starting from the hemostasis phase moving to the inflammatory phase, then to the proliferative phase and finally to the remodeling phase. In the hemostasis phase, chemokines and growth factors aggregate at the wound site to form a clot over the wound. Next in the inflammatory phase, neutrophils and macrophages come to the wound site to clean the site of debris and bacteria. These two phases take approximately 72 hours in total to complete. Following the inflammatory phase, the proliferative phase is involved with replacing the clot formed during the hemostasis phase with connective tissue by encompassing fibroblasts, keratinocytes, and endothelial cells. This phase can last anywhere between several days to weeks. The last phase of the wound healing mechanism is the remodeling phase. In the remodeling phase, type III collagen is replaced with type I collagen and the copious amount of extracellular matrix is degraded. This phase takes between several months to years to complete. Abnormalities to proper progression of this phase can lead to the wound becoming chronic or heal excessively (P.H. Wang, B.S. Huang, H.C. Horng, C.C. Yeh, Y.J. Chen, 2018). In this regard, silk has emerged as a promising material for biomedical applications, particularly in drug delivery, due to its biocompatibility and safety.

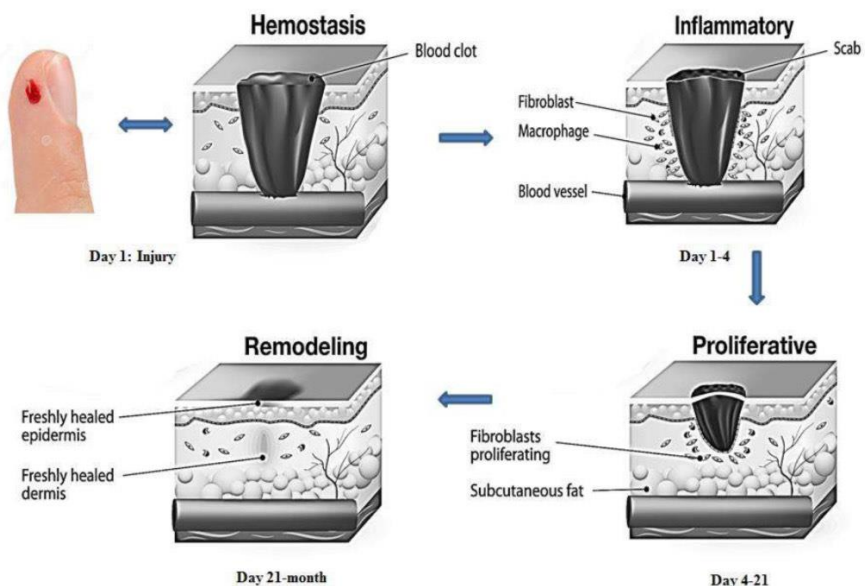


Figure 1. Schematic representation of the wound healing process. (Adapted from Asian Journal of Pharmacy and Pharmacology 2018; 4(2), p.92).

1.3 Silk for Wound Healing

Silk is widely used in biomedical applications for drug delivery due to their safety and biocompatibility. Silk is resourceful to use since it facilitates important mechanisms in the wound healing phases such as during the proliferation phase with cell migration, cell proliferation, angiogenesis, re-epithelization. Multiple studies show that silk combined with silver nanoparticles as an effective wound healing therapy with antibacterial properties (D. Chouhan & B.B. Mandal, 2020).

1.4 Silver Nanoparticles for Wound Healing

Silver nanoparticles are a very promising tool being used in medical application due to their multifunctional physiochemical functions. Silver nanoparticles are used mainly for their antimicrobial properties which are important in tackling issues such as the formation of biofilms

(L. Xu et al., 2020). Studies show that silk patches embedded with silver nanoparticles have efficient antibacterial activity against different types of pathogenic and nonpathogenic bacteria. Silk patches with silver nanoparticles are biocompatible and promote cell migration (P.J. Babu, M. Doble, & A.M. Raichur, 2018). Recent advancements in nanotechnology have paved the way for the development of innovative wound dressings that can improve wound healing outcomes. In addition to silver and silk, the potent antioxidant, cerium oxide, can be used to enhance wound healing.

1.5 Cerium Oxide for Wound Healing

Cerium oxide nanoparticles are beneficial for wound healing as they scavenge ROS allowing the wound to close properly and prevent pathogens from the environment from entering the body through the wound site (H. Cheng et al., 2021). Nanoceria has the ability to penetrate into wound tissue to reduce oxidative stress and oxidative damage to the proteins and cellular membranes in the wound environment (D.A. Pelletier et al., 2010). The antioxidant capabilities of CNPs are determined by the ratio of CNPs carrying different charges — Ce^{3+} to Ce^{4+} which allows for the cell viability variable once cerium oxide penetrates into the cell. The cytotoxicity of nanoceria is highly dependent on the functional groups present on its surface since these functional groups play a large role in determining whether the nanoparticles will be taken up by the cells (D.R. Mullins, 2015). In a study conducted to see the efficacy of engineered Cerium Oxide nanoparticles on bacterial growth, it was shown that Cerium oxide nanoparticles showed growth inhibition toward *E. coli* and *B. subtilis* whereas, *S. oneidensis* growth was not inhibited by the cerium oxide nanoparticles, therefore it would be important to study the bacterial growth and viability on wounds after using our prepared silk patches (D.A. Pelletier et al., 2010).

Cerium oxide nanoparticles also exhibit great UV-protection and therefore it can be used as a coating material for silk for UV-protection (Z. Lu et al., 2014).

Nanocomposites formed with cerium oxide nanoparticles (CNPs) embedded in electrospun silk fiber show promising properties in mechanics including elasticity, elongation, and toughness. The nanocomposite also shows a controlled decay over time allowing it to be a promising tool to use in biomedical applications (I. Kandas et al., 2018). CNPs accelerate the wound healing process by enhancing the proliferation phase of vascular endothelial cells, keratinocytes, and fibroblasts (D.A. Pelletier et al., 2010). Silk fibroin can be used as a carrier to deliver the antioxidant, CNPs. In a one-step desolvation technique used to embed CNPs onto silk to create the nanocomposite, the nanocomposites were shown to efficiently reduce ROS levels and simultaneously enabled imaging of the cells. CNPs utilize a unique redox effect to enhance their antioxidant properties (M. Passi, V. Kumar, & G. Packirisamy, 2020). Oxidative stress contributes to the inability of wounds to properly heal due to an imbalance in redox causing cell and tissue damage (L. Deng et al., 2021). Given the detrimental effects of oxidative stress on wound healing, innovative approaches that target this issue must be investigated to promote optimal healing outcomes.

1.6 A Potential Solution for Enhancing Chronic Wound Healing

We hypothesize that a scaffold created from Silver-Doped Nanoceria (AgCNP) embedded in silk can be beneficial to aid the wound healing process, inhibit inflammation and prevent microorganisms from forming a biofilm over the wound. Current wound healing methods such as intradermal injections are not advantageous to use since they can cause unwanted responses elsewhere in the body other than localizing to the wound site. Silk, however,

has a positive impact on the wound healing effect and can be used as an alternative delivery method to deliver the drugs to the target site rather than intradermal injections since silk's degradability is controllable and it is bioresorbable. As shown in Figure 2, the silk patch can be administered on top of the external wound site to prevent unwanted internal systemic responses. Therefore, it can get absorbed by the body and degrade safely without causing bodily harm. Silk fibroin is notable for being advantageous to use for biomedical wound healing applications due to its biocompatibility.

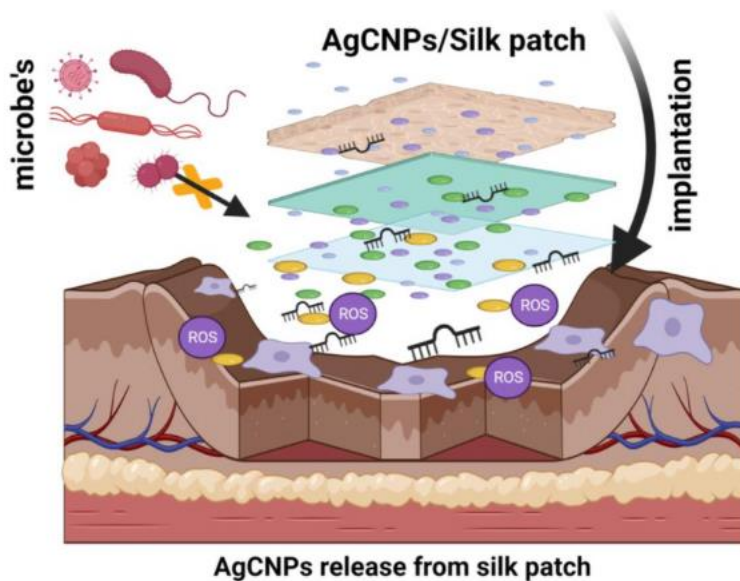


Figure 2. Diagram for proposed silk patch embedded with silver doped nanoceria particles. Silk patch will be placed onto wound environment to prevent the accumulation of microbes and formation of biofilms.

2. EXPERIMENTAL METHODS

2.1 Silk Solution Preparation

The silk scaffolds were prepared by first creating a silk solution and then electrospinning the silk solution using the protocol described by Rockwood et al. (2011). The diagram in Figure 3 illustrates the process of preparing the silk solution through a schematic diagram. The nanoparticles were synthesized by using the protocol described by Neal et. al (2021).

Degumming of Silk

A 3 L glass beaker was used to first boil 2 L of ultrapure water followed by the slow addition of 4.24 sodium carbonate to ensure the solution does not spill over. Once adding the sodium carbonate to the water, gently stir with a spatula to ensure the sodium carbonate has completely dissolved. Immediately after dissolving the required amount of sodium carbonate in water, 5 g of cleaned silk derived from bombyx mori was added into the beaker. This mixture was stirred occasionally to ensure proper dispersion of the silk fibroin and allowed to continue to boil for exactly 30 minutes. It was crucial to remove the fibroin immediately after 30 minutes have passed to ensure reproducibility and prevent fibroin degradation due to excessive boiling. Once removing the fibroin from the solution, the fibroin was rinsed with cold ultrapure water and thoroughly squeezed to remove excess water.

The isolated fibroin was then placed into a 2 L beaker containing 1 L of ultrapure water at room temperature and a stir bar. No heat was added to this step. The fibroin was left in the water for 20 minutes to wash away remaining sodium carbonate and impurities. This washing process was done a total of three times with the water being changed in between each wash.

After the third wash, the silk was removed from the water, squeezed thoroughly to remove excess water, and placed on a sheet of clean aluminum foil under the fume hood to ensure thorough dryness of the fibroin.

This degumming process allows us to remove sericin present in the silk fibroin. This is important since sericin is a glycoprotein that can elicit unwanted immune responses such as allergic reactions in patients (G.H. Altman et al., 2003).

Dissolution of Silk in Lithium Bromide

Once the silk was allowed to completely dry, the amount of silk prepared was weighed. This weight was used to prepare a 20% (wt/vol) solution of silk using 9.3 M lithium bromide (LiBr). The equation used to prepare the 9.3 M LiBr was $(86.85 \text{ g/mol})(9.3 \text{ mol/L})(1 \text{ L}/1000 \text{ mL})(X) = \text{required amount of LiBr in grams}$.

Once preparing the required amount of 9.3 M LiBr, the silk was tightly packed in a small glass beaker and the LiBr was added on top of the silk fibroin. The fibroin was then allowed to completely dissolve in an oven at 60 °C for 4 h. The resulting solution is amber in color, transparent, and highly viscous.

Dialysis and Centrifugation of Silk

The prepared silk solution can cool before performing dialysis to remove the LiBr salt, as it is toxic. The solution is dialyzed against 1 liter of ultrapure water per 12 mL cassette of silk solution. The water for the dialysis was changed over two days over an increasing time interval. The water was changed after the first hour, then the fourth, then that evening, then the next

morning, then that evening, then the following morning for a total of six water changes to ensure successful removal of LiBr.

Though the silk was cleaned, it is possible that there may remain some impurities in the prepares solution, to remove these impurities, the solution is centrifuged and spun at 9,000 r.p.m. (~12,700g) at 4 °C for 20 min. The silk solution is then carefully removed from the centrifuge tubes using a pipette to ensure the pellet of impurities is also not collected.

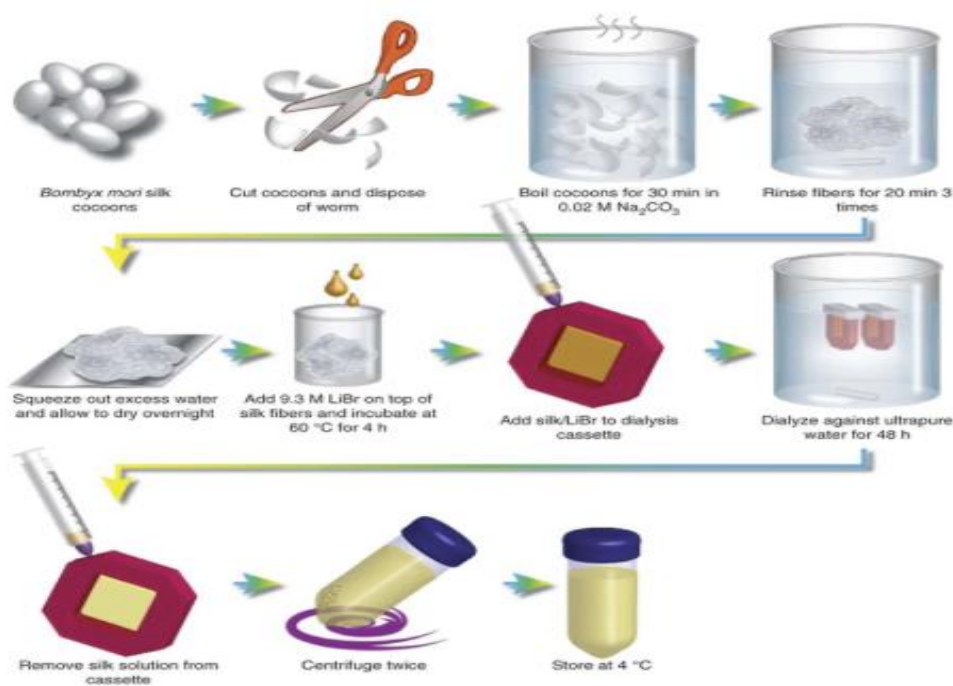


Figure 3. Schematic diagram for silk patch sample preparation. This diagram shows the process of silk degumming, dissolution in LiBr, dialysis, and centrifugation of silk to create silk solution used to make the silk patch.

2.2 Nanoparticle Synthesis

CNPs and AgCNPs were synthesized similarly using a forced hydrolysis process. The nanoparticles were first dissolved in deionized water and vortexed. Then the solution was titrated with 0.4 M of sodium hydroxide. Then the solution was washed three times before being centrifuged and the pellet was resuspended in deionized water. The final concentrations for both CNPs and AgCNPs was 600 $\mu\text{M}/\text{mL}$ (C.J. Neal et al., 2021).

2.3 Silk Composite Preparation Using Electrospinning

Electrospinning was used to produce the silk patches. First, silk solution with no nanoparticles added was mixed with 5% (wt/vol) PEO solution, and drawn into a 10 mL syringe, which was then loaded onto the electrospinning machine. This process allowed for the construction of the control silk patch. The silk patches embedded with CNPs and AgCNPs were constructed in a similar manner, however, the prepared nanoparticles were added to the respective silk solution before electrospinning. The parameters used for the electrospinning process were constant for the three different types of silk composites created including silk control, silk with CNP, and silk with AgCNP. The parameters include spinning at a voltage of 18 eV, 10 cm distance between needle and drum collector, and rotations at 2000 rpm (Rockwood et al., 2011).

2.4 Nanoparticle Characterization

In this laboratory experiment, X-ray photoelectron spectroscopy (XPS), UV/Vis spectroscopy, and Transmission Electron Microscopy (TEM) imaging were used to characterize CNPs and AgCNPs synthesized. XPS is an ultra-high vacuum technique that allows us to quantitatively measure the elemental composition of the surface composition of our

nanoparticles (R.R. Mather, 2009). UV/VIS characterization was done using UV/Vis Spectroscopy. UV/Vis Spectroscopy allows us to analyze the amount of UV or visible light that is absorbed by different samples (J. Tom, 2021). TEM imaging is an imaging tool that allows us to confirm the structural characterization of molecules at a nanoscale. TEM utilizes a beam of electrons that are accelerated and focused by electromagnetic fields (S.J. Pennycook, 2005).

2.5 Silk Composites Characterization

The silk composites were also characterized using XPS. Additionally, an MTT assay and Scratch assay were performed to check for the effects of the silk composites containing the nanoparticles on cell growth. The MTT Assay was conducted following the protocol described by C. El Chzaoui et al., to study the cytotoxicity of the silk composites on the cells. The cells were incubated over a course of 3 days. Following incubation, the cells were removed from the medium and stained with red and green dyes to visualize the number of live cells and dead cells. Finally, a scratch assay was conducted using the protocol given by C.C. Liang et al. in which a scratch was made on the cell to quantify the progression of wound healing under the administration of the silk composites. The purpose of a scratch assay is to create a controlled, artificial "wound" or gap in a confluent cell monolayer and to observe and measure the migration of cells into the gap over time.

3. RESULTS AND DISCUSSION

3.1 Sample Preparation

The silk solution was prepared strictly using the parameters described in the protocol used to increase reproducibility (Rockwood et al., 2011). The nanoparticles, AgCNP and CNPs, were synthesized based on aqueous chemistry (Neal et al.). Figure 4 shows the appearance of the silk scaffold constructed using the electrospinning technique. All three silk scaffolds produced had the same appearance without the aid of a microscope. To confirm that the nanoparticles were successfully embedded onto the silk scaffold during the electrospinning process and not lost elsewhere, multiple nanoparticles characterizations were conducted.

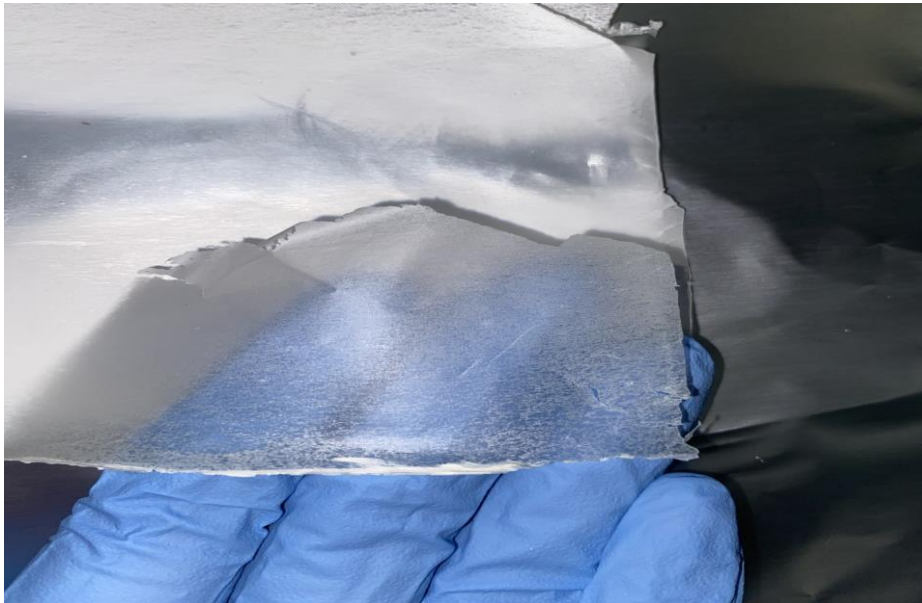


Figure 4. Control silk patch created using electrospinning. Three scaffolds, one control silk patch with no nanoparticles added, one silk patch with CNPs, and one silk patch with AgCNPs were created. They all appeared identically and formed a thin paper like sheet.

3.2 Nanoparticle Characterization Results

XPS Characterization

The peaks on the XPS graph indicate whether the nanoparticles were present in the materials we tested for (R.R. Mather, 2009). The peaks seen on the graphs in Figure 5, which indicate the presence of our nanoparticles are very intense indicating a high concentration of nanoparticle present in the sample. This allows us to confirm that most of the nanoparticles inducted into the silk solution before electrospinning successfully embedded onto the fiber mat.

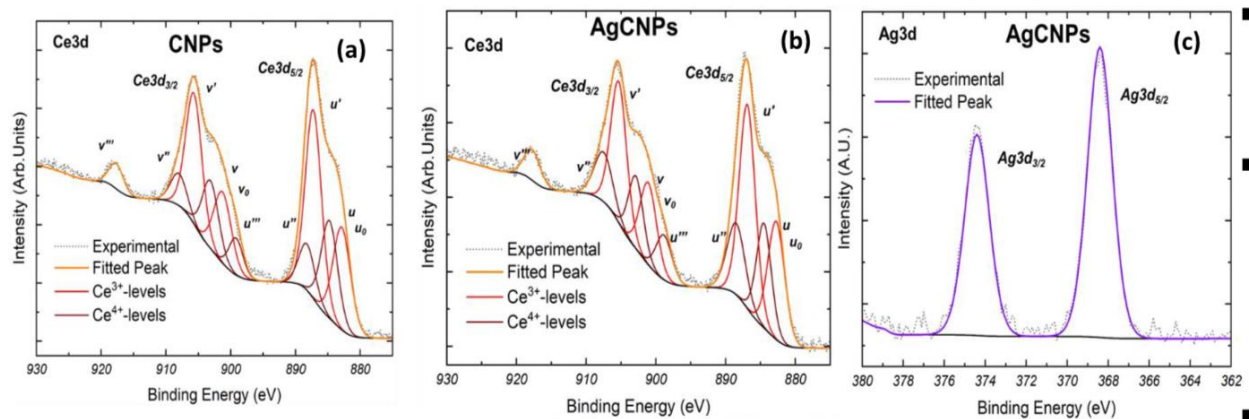


Figure 5. Results of XPS analysis for CNPs and AgCNPs. If the cerium in the CNPs is present in its trivalent form (Ce³⁺), then a peak will be observed at binding energies of 899.7 and 904.2 eV. If it is present in, then the peaks of Ce³⁺ 3d_{3/2} (at binding energies of 899.7 and 904.2 eV) and Ce³⁺ 3d_{5/2} (881.5 and 885.9 eV).

UV/Vis Spectroscopy

UV/Vis spectroscopy data further allows us to confirm the presence of our nanoparticles of interest. As silver and cerium oxide are discovered to absorb light at specific wavelengths, peaks present at the wavelength can be used to quantify the presence of the nanoparticles of interest (J. Tom, 2021). In the graphs shown in Figure 6, an intense peak is seen at where we would expect CNPs and AgCNPs to absorb light. Cerium 3 produces a peak for an absorbance value within the 230 to 260 nm range (E. Heckert, A. Karakoti, S. Seal, W. Self, 2009). This further confirms the successful retention of nanoparticles in our silk composites.

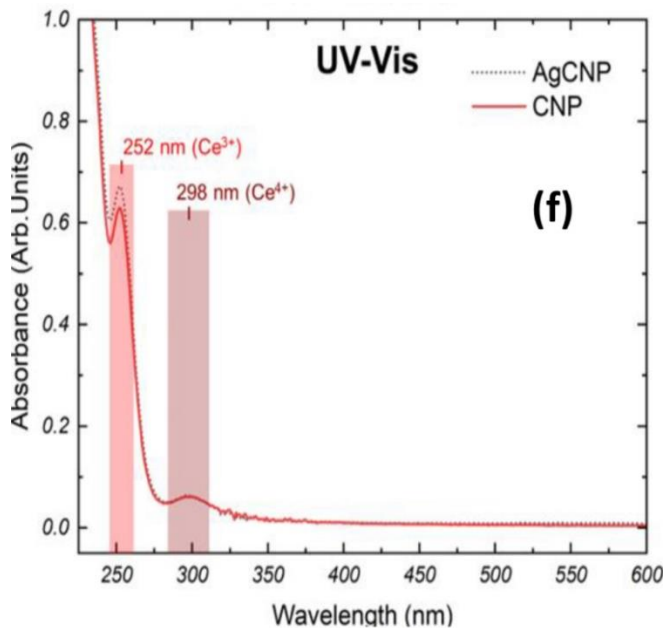


Figure 6. Results of UV/Vis analysis for CNPs and AgCNPs. The peaks are observed at the expected absorbance wavelengths for CNP and AgCNP. UV/Vis characterization confirmed the presence of both Ce³⁺ and 4+ valence states since Ce³⁺ produces a peak at a wavelength of 252

nm and Ce^{4+} produces a peak at a wavelength of 298 nm both of which were observed in the analysis.

TEM Imaging

TEM Imaging was used to confirm the size and morphology of CNPs and AgCNPs. AgCNPs are bigger in size compared to CNPs. The images obtained shown in Figure 7, show the presence of CNP and AgCNP by confirming the morphology of the nanoparticles found in the silk composite. TEM imaging hence allows us to further confirm the identity of the nanoparticles present (S.J. Pennycook, 2005).

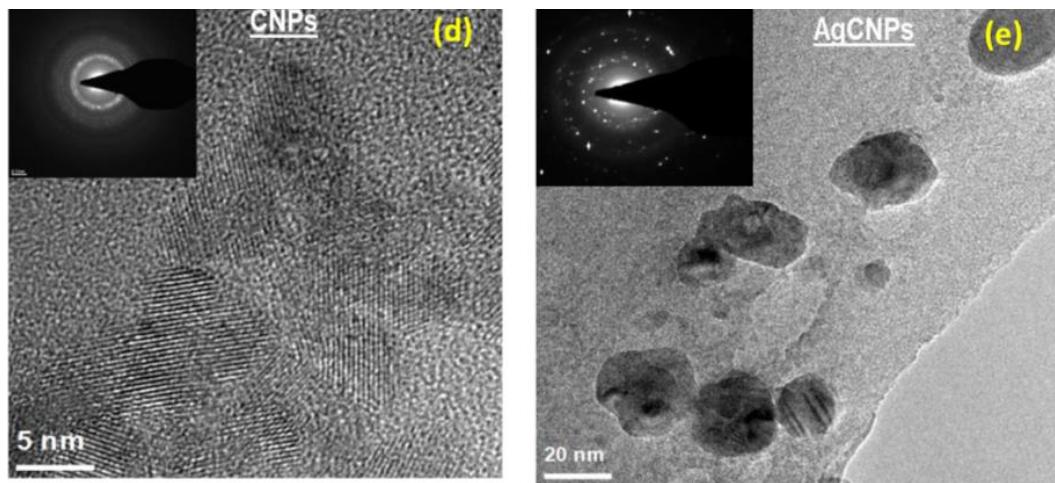


Figure 7. TEM Images for CNP and AgCNP. TEM Imaging allows us to confirm the size of the nanoparticles. CNPs are expected to be approximately 5 nm, while AgCNPs are expected to be 20 nm.

3.3 Silk Composites Characterization Results

XPS Characterization

As confirmed by the results presented in Figure 8, the peaks on the XPS graph indicate the expected bonds observed in silk composites. By running an XPS on silk, we were able to understand the surface chemistry of silk.

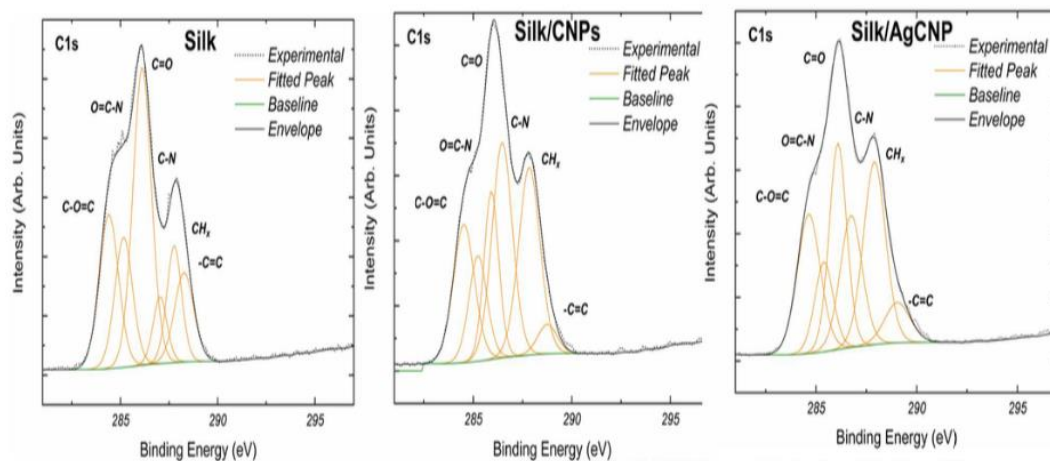
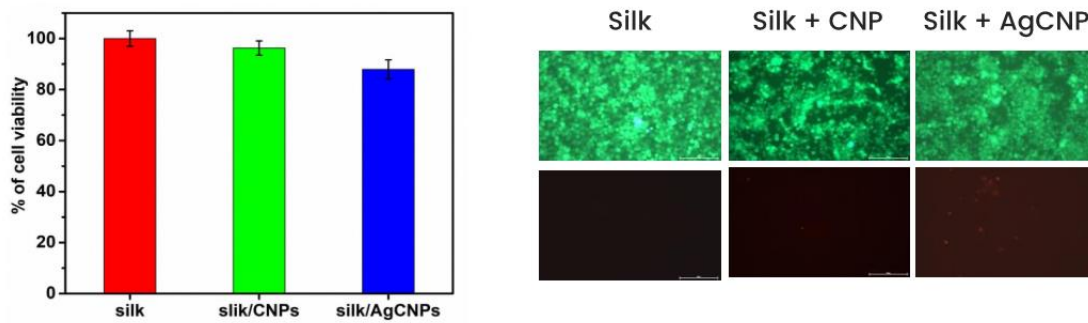


Figure 8. Results of XPS analysis for Silk and Silk Composite. Allows for the confirmation of silk since peaks were seen for functional groups commonly found in silk. This includes a peak at 284.4 eV for $-C=C$, at 285 eV for CH_x , at 285.9 eV for to the $C-N$ bond, at 287.5 eV for $-C=O$, at 288 eV for to $O=C-N-$, and at 289.5 eV for $-O-C=O$.

MTT Assay

The MTT Assay conducted indicated the cell viability of the cells administered with the silk control, silk with CNP, and silk with AgCNP. A green colored dye which is taken up by live and dead cells, and a red dye taken up by dead cells only was used to visualize the quantify and ratify the amount of live cells to dead cells (C. El Ghzaoui et al., 2018). As seen in Figure 9, all three environmental conditions show a percentage of cell viability. However, though it is not a significantly big decrease, cells that were administered with CNPs and AgCNPs showed a

smaller percentage less cell viability than the silk control. A potential explanation can be the toxicities and side effects associated with the prolonged utilization of silver. Studies have shown that increased exposure to silver nanoparticles can cause mitochondrial damage and amplified production of ROS species. However, the cerium oxide can be beneficial in combatting the effects of silver toxicity (P.V. AshaRani, G. Low Kah Mun, M.P. Hande, & S. Valiyaveetil, 2009). Future studies should conduct cell viability studies using different concentrations of silver nanoparticles to optimize a quantity that is both highly safe and efficient.



Tests for Cell Viability

Figure 9. MTT Assay was conducted using all three silk scaffolds. The MTT Assay shows a high percentage of cell viability for all three silk composites.

Scratch Assay

Scratch assays are commonly used to analyze the tissue repair capacity of cells. This method allows us to observe and analyze the motion of cells over a short period of time after an initial scratch is made on the cells monolayer (S.T. Johnston, M.J. Simpson, & D.L.S. McElwain, 2014). The results from Figure 10 show the scratch assay that was conducted on macrophage

cells. The cells were incubated in one of three environments, with either the silk control, silk with CNP, or silk with AgCNP, for a period of three days. After the three-day period, the cells were observed to visualize how much they have progressed in closing the gap created by the scratch. The scratch assay revealed excellent cell proliferation, suggesting that our silk composite has the potential to promote accelerated wound healing. The scratch assay indicates that the cells have a high migratory capacity and ability to close the wound site. This indicates that silk composites can be a novel approach to treat chronic wounds.

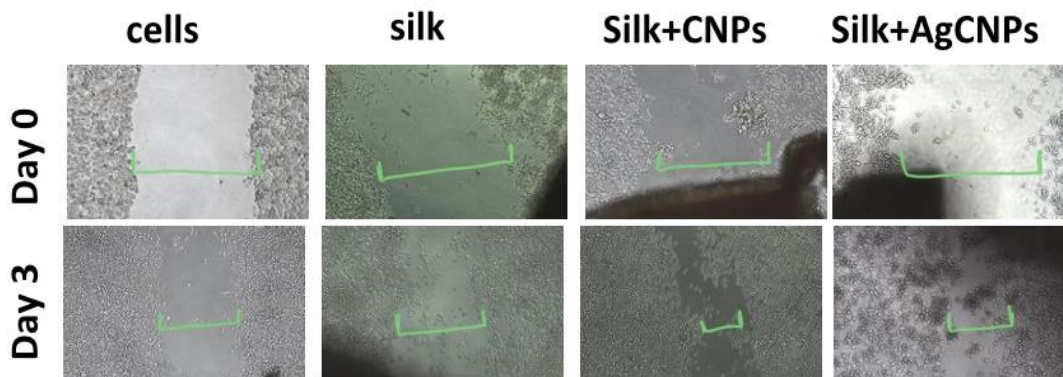


Figure 10. Scratch Assay is conducted on all three silk composites. Excellent cell proliferation was seen in the scratch assay conducted, indicating the potential for enhanced wound healing with our silk composite.

The creation of this silk scaffold embedded with silver doped nanoceria has shown to have potential applications in tissue engineering and drug delivery (N. Kasoju & U. Bora, 2012). The characterization results presented in this context provide valuable insights into the composition and properties of the scaffolds and can aid in optimizing their design and function for specific applications.

In this study, the silk solution used for both the control silk patch and silk composites was prepared with the same wt/vol% concentration (9%) to minimize any concentration-dependent effects on the results (Rockwood et al., 2018). The successful synthesis of the nanoparticles and their incorporation into the silk scaffold was confirmed through characterization results.

The MTT assay, which evaluates cell viability, was conducted to assess the biocompatibility of the silk composites (C. El Ghzaoui et al., 2018). The results of the assay indicated high cell viability, indicating that the silk composites are safe for use in biomedical applications. Additionally, the scratch assay conducted in this study demonstrated excellent cell proliferation, indicating that the silk composites may have the potential to enhance tissue regeneration.

However, a limitation of this experiment was the long production time required for the silk scaffold creation. Although this study showed promising results, further research must be conducted to investigate the long-term efficacy of the silk composite. Additional studies must also be conducted to investigate potential methods for optimizing the production time of the silk scaffold to make it more practical for clinical applications. Overall, this study provides valuable insights into the potential use of silk composites for biomedical applications and highlights the need for further research in this area.

In future directions, miRNA 146-a could be used to enhance the impacts of the silk scaffold. By creating a silk patch containing miRNA 146-a and AgCNP, many difficulties chronic wound healing faces can be tackled. miRNA is a crucial component as it attenuates excess inflammatory gene expression to prevent chronic inflammation. AgCNPs are used as they

have both antimicrobial and antioxidant properties to scavenge harmful ROS species at the wound site and can also modify silk for UV protection. miRNA 146-a is beneficial to use in wound healing therapy applications as it attenuates the inflammatory gene expression to prevent chronic inflammation and promotes angiogenesis. miRNA 146-a also inhibits pro inflammatory pathways. miRNA plays an essential role of regulation in cell physiology and pathology. microRNA-146a gets dysregulated in diabetic wounds when applied which can be fixed with the loading of miRNA onto cerium oxide nanoparticles helps prevent this (Z. Meng, D. Zhou, Y. Gao, M. Zeng, & W. Wang, 2018). Using cerium oxide in conjugation with miRNA 146a can increase collagen production in the wound site which ameliorates the proliferative phase. It also lowers inflammation and oxidative stress on the wound site allowing for the wound to close faster and heal (L.C. Dewberry et al., 2022).

4. CONCLUSION

The purpose of this experiment was to investigate the potential therapeutic applications of a silk scaffold that contains silver doped nanoceria for chronic wound healing. The choice of materials was made based on their antibacterial and antimicrobial properties, which could be beneficial in combating biofilm formation in chronic wounds. Silk, being a biocompatible material, could be a safer option compared to other treatments available in the market for chronic wound healing. The results of the study showed promising outcomes, where the silk scaffold embedded with silver doped nanoceria was able to reduce the size of wounds, as seen in the scratch assay. Additionally, the MTT assay demonstrated that the scaffold was safe to administer to cells, as it showed high cell viability. However, further studies need to be conducted over an extended period to evaluate the potential side effects and toxicities of silver and cerium oxide. Overall, this study provides a beginning level understanding of the novel approach of using this nanoparticle-mediated drug therapy for chronic wound healing. If proven safe and effective in future studies, this therapy could be a valuable tool in treating chronic wounds and improving the quality of life for patients suffering from such conditions.

5. REFERENCES

- Altman, G. H., Diaz, F., Jakuba, C., Calabro, T., Horan, R. L., Chen, J., ... & Kaplan, D. L. (2003). Silk-based biomaterials. *Biomaterials*, 24(3), 401-416. [https://doi.org/10.1016/S0142-9612\(02\)00353-8](https://doi.org/10.1016/S0142-9612(02)00353-8)
- Anderson, K., & Hamm, R. L. (2014). Factors That Impair Wound Healing. *The journal of the American College of Clinical Wound Specialists*, 4(4), 84–91. <https://doi.org/10.1016/j.jccw.2014.03.001>
- AshaRani, P. V., Low Kah Mun, G., Hande, M. P., & Valiyaveetil, S. (2009). Cytotoxicity and genotoxicity of silver nanoparticles in human cells. *ACS Nano*, 3(2), 279-290. <https://doi.org/10.1021/nn800596w>
- Babu, P. J., Doble, M., & Raichur, A. M. (2018). Silver oxide nanoparticles embedded silk fibroin spuns: Microwave mediated preparation, characterization and their synergistic wound healing and anti-bacterial activity. *Journal of colloid and interface science*, 513, 62–71. <https://doi.org/10.1016/j.jcis.2017.11.001>
- Cheng, H., Shi, Z., Yue, K., Huang, X., Xu, Y., Gao, C., Yao, Z., Zhang, Y. S., & Wang, J. (2021). Sprayable hydrogel dressing accelerates wound healing with combined reactive oxygen species-scavenging and antibacterial abilities. *Acta biomaterialia*, 124, 219–232. <https://doi.org/10.1016/j.actbio.2021.02.002>
- Chouhan, D., & Mandal, B. B. (2020). Silk biomaterials in wound healing and skin regeneration therapeutics: From bench to bedside. *Acta biomaterialia*, 103, 24–51. <https://doi.org/10.1016/j.actbio.2019.11.050>

- Costerton JW, Stewart PS, Greenberg EP. Bacterial biofilms: a common cause of persistent infections. *Science*. 1999 May 21;284(5418):1318-22. doi: 10.1126/science.284.5418.1318. PMID: 10334980.
- Darvishi, S., Tavakoli, S., Kharaziha, M., Girault, H. H., Kaminski, C. F., & Mela, I. (2022). Advances in the Sensing and Treatment of Wound Biofilms. *Angewandte Chemie (International ed. in English)*, 61(13), e202112218. <https://doi.org/10.1002/anie.202112218>
- Deng, L., Du, C., Song, P., Chen, T., Rui, S., Armstrong, D. G., & Deng, W. (2021). The role of oxidative stress and antioxidants in diabetic wound healing. *Oxidative Medicine and Cellular Longevity*, 2021, Article ID 8852759, 11 pages. <https://doi.org/10.1155/2021/8852759>
- Diban, F., Di Lodovico, S., Di Fermo, P., D'Ercole, S., D'Arcangelo, S., Di Giulio, M., & Cellini, L. (2023). Biofilms in Chronic Wound Infections: Innovative Antimicrobial Approaches Using the In Vitro Lubbock Chronic Wound Biofilm Model. *International journal of molecular sciences*, 24(2), 1004. <https://doi.org/10.3390/ijms24021004>
- Dewberry, L. C., Niemiec, S. M., Hilton, S. A., Louiselle, A. E., Singh, S., Sakthivel, T. S., Hu, J., Seal, S., Liechty, K. W., & Zgheib, C. (2022). Cerium oxide nanoparticle conjugation to microRNA-146a mechanism of correction for impaired diabetic wound healing. *Nanomedicine : nanotechnology, biology, and medicine*, 40, 102483. <https://doi.org/10.1016/j.nano.2021.102483>
- El Ghzaoui, C., Neal, C. J., Kolanthai, E., Fu, Y., Kumar, U., Hu, J., Zgheib, C., Liechty, K. W., & Seal, S. (2018). Assessing the bio-stability of microRNA-146a conjugated nanoparticles via electroanalysis. *Nanoscale*, 10(6), 2706-2715. doi: 10.1039/C7NR07580F

- Garg, S., Garg, A., Shukla, A., Dev, S., & Kumar, M. (2018). A review on Nano-therapeutic drug delivery carriers for effective wound treatment strategies. *Asian Journal of Pharmacy and Pharmacology*, 4(2), 90-101. <https://doi.org/10.31024/ajpp.2018.4.2.1>
- Gil, E. S., Panilaitis, B., Bellas, E., & Kaplan, D. L. (2013). Functionalized silk biomaterials for wound healing. *Advanced healthcare materials*, 2(1), 206–217. <https://doi.org/10.1002/adhm.201200192>
- Guo, S., & Dipietro, L. A. (2010). Factors affecting wound healing. *Journal of dental research*, 89(3), 219–229. <https://doi.org/10.1177/0022034509359125>
- Heckert, E., Karakoti, A., Seal, S., & Self, W. T. (2008). The role of cerium redox state in the SOD mimetic activity of nanocerium. *Biomaterials*, 29(18), 2705–2709. doi: 10.1016/j.biomaterials.2008.03.014. PMID: PMC2396488, NIHMSID: NIHMS49835, PMID: 18395249.
- Johnston, S. T., Simpson, M. J., & McElwain, D. L. S. (2014). How much information can be obtained from tracking the position of the leading edge in a scratch assay? *Journal of the Royal Society Interface*, 11(98), 20140325. <https://doi.org/10.1098/rsif.2014.0325>
- Kandas, I., Shehata, N., Hassounah, I., Sobolciak, P., Krupa, I. Sr., & Lewis, R. (2018). Optical fluorescent spider silk electrospun nanofibers with embedded cerium oxide nanoparticles. *Journal of Nanophotonics*, 12(2), 026016. <https://doi.org/10.1117/1.JNP.12.026016>
- Kasaju, N., & Bora, U. (2012). Silk Fibroin in Tissue Engineering. *Advanced Healthcare Materials*, 1(4), 393-412. <https://doi.org/10.1002/adhm.201200097>

- Liang, C. C., Park, A., & Guan, J. L. (2007). In vitro scratch assay: A convenient and inexpensive method for analysis of cell migration in vitro. *Nature Protocols*, 2, 329–333.
<https://doi.org/10.1038/nprot.2007.30>.
- Lu, Z., Mao, C., Meng, M., Liu, S., Tian, Y., Yu, L., Sun, B., & Li, C. M. (2014). Fabrication of CeO₂ nanoparticle-modified silk for UV protection and antibacterial applications. *Journal of colloid and interface science*, 435, 8–14. <https://doi.org/10.1016/j.jcis.2014.08.015>
- Mather, R. R. (2009). Surface modification of textiles by plasma treatments. In Q. Wei (Ed.), *Surface modification of textiles* (pp. 543-576). Woodhead Publishing.
- Meng, Z., Zhou, D., Gao, Y., Zeng, M., & Wang, W. (2018). miRNA delivery for skin wound healing. *Advanced drug delivery reviews*, 129, 308–318. <https://doi.org/10.1016/j.addr.2017.12.011>
- Mullins, D. R. (2015). The surface chemistry of cerium oxide. *Surface Science Reports*, 70(1), 42-85.
<https://doi.org/10.1016/j.surfrep.2014.12.001>.
- Neal, C. J., Tobin, M. J., Zhang, Y., Peng, J., Lin, Z., Gelfand, M. P., ... & Raghavan, S. R. (2021). Metal-mediated nanoscale cerium oxide inactivates human coronavirus and rhinovirus by surface disruption. *ACS Nano*, 15(9), 14544-14558. <https://doi.org/10.1021/acsnano.1c04679>
- Passi, M., Kumar, V., & Packirisamy, G. (2020). Theranostic nanozyme: Silk fibroin based multifunctional nanocomposites to combat oxidative stress. *Materials Science and Engineering: C*, 107, 110255. <https://doi.org/10.1016/j.msec.2019.110255>
- Pelletier, D. A., Suresh, A. K., Holton, G. A., McKeown, C. K., Wang, W., Gu, B., Mortensen, N. P., Allison, D. P., Joy, D. C., Allison, M. R., Brown, S. D., Phelps, T. J., & Doktycz, M. J. (2010).

Effects of engineered cerium oxide nanoparticles on bacterial growth and viability. *Applied and environmental microbiology*, 76(24), 7981–7989. <https://doi.org/10.1128/AEM.00650-10>

Pennycook, S.J. (2005). Transmission electron microscopy. In F. Bassani, G.L. Liedl, & P. Wyder (Eds.), *Encyclopedia of condensed matter physics* (pp. 444-453). Elsevier.

Pollini, M., & Paladini, F. (2020). Bioinspired Materials for Wound Healing Application: The Potential of Silk Fibroin. *Materials* (Basel, Switzerland), 13(15), 3361. <https://doi.org/10.3390/ma13153361>

Rockwood, D. N., Preda, R. C., Yücel, T., Wang, X., Lovett, M. L., & Kaplan, D. L. (2011). Materials fabrication from *Bombyx mori* silk fibroin. *Nature protocols*, 6(10), 1612–1631. <https://doi.org/10.1038/nprot.2011.379>

Tom, J. (2021, June 30). UV-Vis Spectroscopy: Principle, Strengths and Limitations and Applications. *Technology Networks*. <https://www.technologynetworks.com/analysis/articles/uv-vis-spectroscopy-principle-strengths-and-limitations-and-applications-349865>

Wang, P. H., Huang, B. S., Horng, H. C., Yeh, C. C., & Chen, Y. J. (2018). Wound healing. *Journal of the Chinese Medical Association : JCMA*, 81(2), 94–101. <https://doi.org/10.1016/j.jcma.2017.11.002>

Xu, L., Wang, Y. Y., Huang, J., Chen, C. Y., Wang, Z. X., & Xie, H. (2020). Silver nanoparticles: Synthesis, medical applications and biosafety. *Theranostics*, 10(20), 8996–9031. <https://doi.org/10.7150/thno.45413>